Stress evaluation of a bicycle crank arm connection using BEM

C. J. Hoff, R. E. Dippery & J. Knapp
Department of Mechanical Engineering
Kettering University, USA

Abstract

An interesting problem encountered in teaching mechanics of solids and design of mechanical components is the determination of the stresses in the connection between two components such as a bicycle spindle and crank arm. The problem generally posed to students in class is to determine the maximum stresses at the base of the crank arm. In the real-world of design, the stresses developed at the connection of the spindle and crank arm are of major interest. A question arises as to how to determine the stress concentration in the crank arm due to the presence of an interference fit with the spindle. This paper discusses how the BEM was used to evaluate such a situation, with the results compared to classical methods.

Introduction

The impetus for this paper was an example problem used in a Machine Component Design course, to review Solid Mechanics principles. The problem was to calculate stresses and deflections in a bicycle crank arm assembly. Nominally, this is a good review problem because: (a) the students can relate to this simple device that they all encounter in their every day life (and theoretically, they will have more motivation to pay attention) and (b) the problem offers the opportunity to review topics such as: Free Body Diagrams, Shear and Bending Moment Diagrams, Combined Stress Analysis (Bending Stress and Torsional Stress), Principle Stresses, Torsional Stress in a Non-Round Cross Section (a new concept for most students), and Beam Deflection.

The problem also offers the opportunity to bring in design concepts. For example a simple question such as, "What is the appropriate design load?", leads

to a discussion of anthropomorphic data ("What size are the people who will be riding the bike?"), load cases ("How will the people be using the bike?", "How will forces be applied?", "Will there be impact?"), and factor of safety ("Is there a potential for people to be injured do to design failure?"). The problem is an excellent lead-in into a discussion of static and fatigue failure theories.

It was also thought that the problem would provide an opportunity to discuss the concept of Stress Concentration Factors (due to the presence of a hole through the crank arm). However, it was quickly realized that situation was much different than cases normally made available in mechanics textbooks and handbooks and that a numerical solution using FEA or BEM methods would be required. Ultimately, both methods were used. This paper summarizes the important results of this study.

Background

There are a number of methods used to manufacture bicycle crank arm assemblies. One common method, used on very low end bicycles, is to make the crank arm out of a single solid round steel bar, bent to the appropriate shape. The crank arm is snaked through the bottom bracket of the bicycle frame, a bearing is slid over the crank arm from either side, and the assembly is held in place by the cap and nut.

On very high-end bicycles the crank arm and shaft through the bottom bracket (called the spindle) are made out of separate pieces. The spindle and bearing come as an assembly, referred to as a bottom bracket. The spindle is often made of titanium alloy and is splined to accept the crank arm. Crank bolts are used to hold the crank on the spindle.

On mid-range bicycles the crank arm and spindle are also made as two

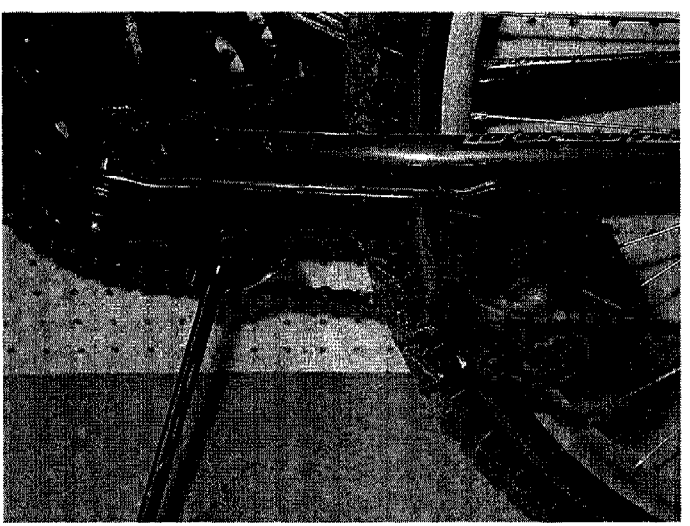

Figure 1: Bicycle crank arm from a mid-range bicycle.

separate pieces. However, instead of being splined, the end of the spindle is tapered and threaded. The crank arm is held in place by an interference fit, created when a nut is tightened to press the crank arm onto the spindle. An example of this design is shown in Figure 1. This is the design which is the focus of this paper.

A simplified drawing of one such crank arm is shown in Figure 2. The thickness of the crank arm is 20-mm. Note that the details at the pedal end of the crank arm have been neglected, because the focus of this study is on the stress concentrations associated with the spindle hole.

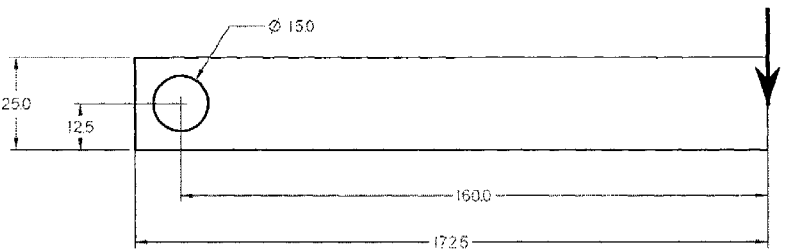

Figure 2: A simplified drawing of the mid-range bicycle crank arm.

Analytical Solution

For the initial study, the crank arm was assumed to be two-dimensional and the torsional load caused by the load application on the pedal was neglected. Also, in the initial study, the stresses caused by the interference fit were neglected. This means that the only stress at the hole will come from the bending load.

The pedal load was assumed to be 1000-N, so that the bending moment at the spindle hole is 160 N-m. The bending stress at the hole is found from:

$$\sigma = \frac{My}{I} \tag{1}$$

where, M is the bending moment, y is the location from the neutral axis, and I is the area moment of inertia for the cross section.

$$I = \frac{1}{12} b\left(h^3 - d^3\right) = 2.042 \times 10^4 mm^4 \tag{2}$$

where, b is the crank arm thickness (20-mm), h is the crank arm height (25-mm), and d is the diameter of the hole (15-mm). The nominal values for stress at the cross section through the hole are summarized in Table 1.

Table 1 Summary of nominal stress values.

Location	y (mm)	σ_{nom} (MPa)
Top of hole	7.5	58.8
Top of crank arm	12.5	98.0

It would be expected that the stress at the top of the hole would be increased by a stress concentration factor due to the geometric discontinuity of the hole. Data for the stress concentration factor in this particular arrangement are not available. If the crank arm could be modeled as a cantilever beam fixed at left-hand end of the arm (relative to orientation in Figure 2) the stress concentration factor can be estimated from data for a plate with a hole in pure bending (see Figure 3).

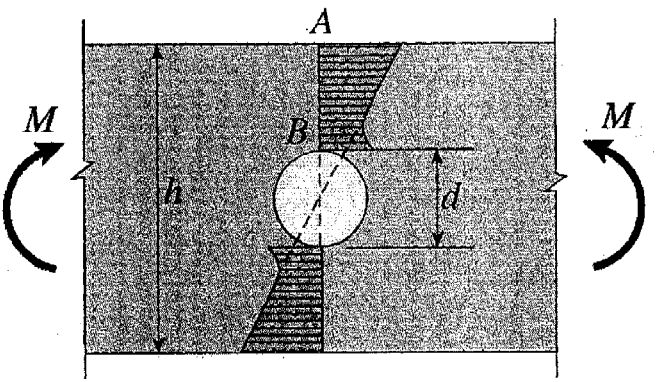

Figure 3: Stress concentrations for a flat plate with a hole in pure bending (Gere [1]).

The stress concentration factor for this orientation is not routinely found in the standard reference books (i.e. Solid Mechanics texts, Machine Design texts, and Machinery Handbooks). Gere [1] reports "extensive investigations have shown that the stress at the edge of the hole is approximately twice the nominal stress at that point." With this constraint condition, the stress at the top edge of the hole would be:

$$\sigma_{\max} = K_t \sigma_{nom} = 2(58.8MPa) = 117.6MPa \tag{3}$$

However, the assumption of a fixed-end constraint is not appropriate for this loading situation. This can be seen clearly by considering a force-flow diagram. Figure 4 shows such a diagram for the fixed-end boundary condition. All the force lines pass through the area between the hole and the top edge of the crank as they 'flow' to the end constraint. The high number of force-flow lines that pass through this small area leads to the stress concentrations shown in Figure 3.

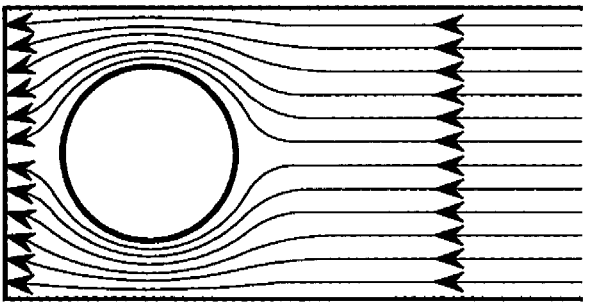

Figure 4: Force-flow diagram for fixed-end boundary condition.

A better model for this situation is to constrain the crank arm at the spindle hole. The interference fit at the spindle hole creates frictional forces that directly constrain the edges of the hole. The force-flow diagram for this situation is shown in Figure 5. This figure suggests that the stress induced in the region between the spindle hole and the edge of the crank be substantially lower than indicated by the nominal values in Table 1. This is because much of the force flows directly into the spindle and does not travel through the region.

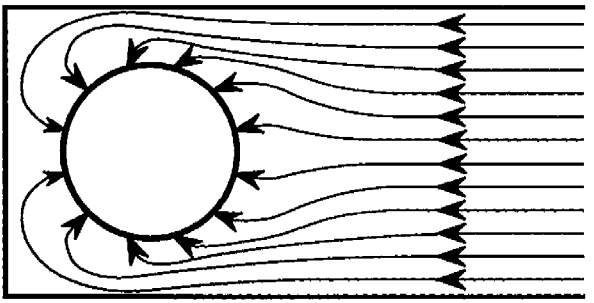

Figure 5: Force-flow diagram for fixed-hole boundary condition.

BEM Modeling

As indicated in the previous section, there is no readily available analytical model for the crank arm/spindle interface. The force-flow approach predicted a solution that was not intuitively obvious (*i.e.*, that there was no stress concentration). Consequently, computer methods were developed using the boundary element method.

A portion of the boundary element mesh in the vicinity of the hole, along with the fixed-hole boundary constraint is shown in Figure 6. The fixed-end boundary condition was also analyzed using the same mesh, in order to compare the results to the known analytical solution. The fixed-hole constraint was a simplified version of the actual load constraint. The full DOF constraint applied

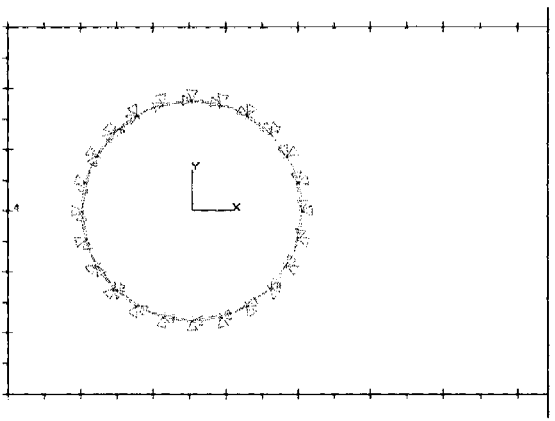

Figure 6: BEM mesh showing fixed-hole boundary condition

to the edge of the spindle hole is a reasonable approximation to the condition of infinite friction along the spindle/crank interface. It should be noted that this initial model neglects the contact stresses associated with the interference fit. This effect will be considered in a later study.

The applied force was a 1000-N load in the negative y-direction, applied at a distance of 160-mm from the hole, as indicated in Figure 2. The x-component bending stress for the fixed-end boundary constraint is shown in. The results indicate a stress concentration at the top edge of the hole as expected. The maximum stress at this point was found to be 120.4 MPa, indicating a stress concentration factor of 2.05.

The BEM results for the fixed-hole boundary condition are shown in Figure 8. The results seem to verify the force-flow prediction, as there appears to be little stress across the region between the top of the spindle hole and the top of

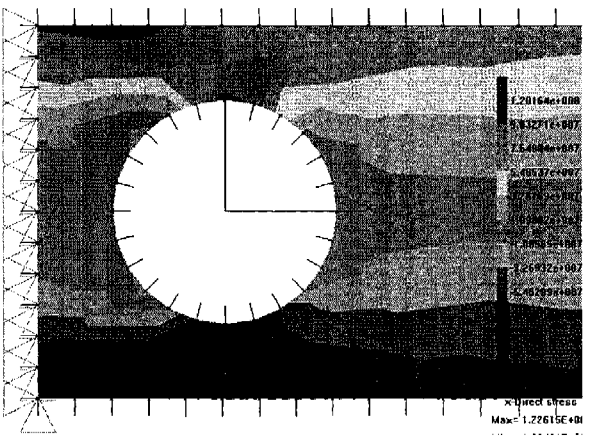

Figure 7: BEM results showing σ_x for fixed-end boundary condition.

the crank. The high stress regions at ±45° from the leading edge of the hole also seem to support the hypothesis that much of the load is transmitted directly to the spindle at the friction interface. The stress at the top of the spindle hole was found to be 2.2 MPa, which is only 3.7% of the nominal value of stress at that point predicted by the analytical solution.

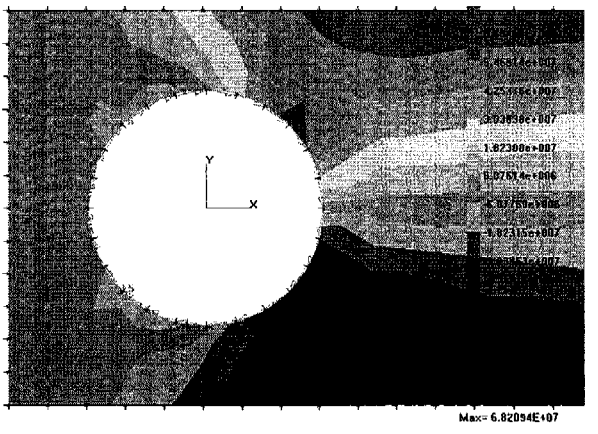

Figure 8: BEM results showing σ_x for fixed-hole boundary condition.

FEA Modeling

To confirm the results of the BEM study, the problem was also solved (with considerably more effort) using the finite element method. A portion of the FEA mesh is shown in Figure 9.

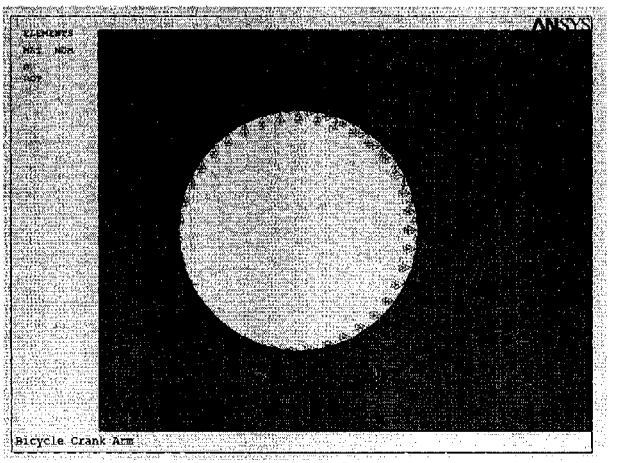

Figure 9: A portion of the FEA mesh

The FEA result for the fixed-end boundary constraint is shown in Figure 10. The result is consistent with the BEM study. Here the maximum stress at the top edge of the hole was found to be 106.0 MPa, indicating a stress concentration factor of 1.80.

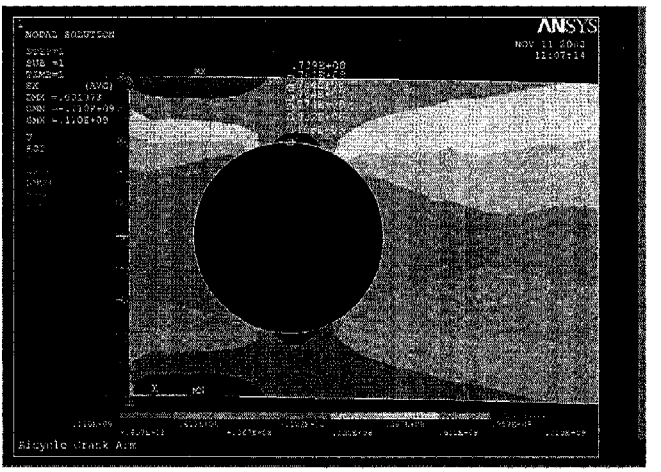

Figure 10: FEA results showing σ_x for fixed-end boundary condition

The FEA result for the fixed-hole boundary constraint is shown in Figure 11 and again the result is very similar to the BEM study. The stress at the top of the spindle hole was found to be 2.1 MPa, which was very close to the BEM value of 2.2 MPa.

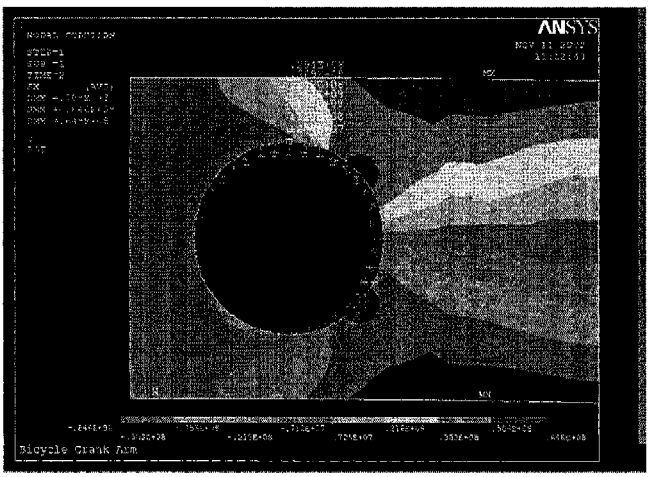

Figure 11: FEA results showing σ_x for fixed-hole boundary condition

Discussion

The variation of the x-component (bending) stress across the region between the hole and the top of the crank for each method is shown in Figure 12. Again, it is seen that the BEM and FEA solutions are in very close agreement, although the correlation between the two methods seems higher for the fixed-hole boundary condition than for the fixed-end boundary condition. For the latter case, there seems to be some deviation between the two methods near the surface of the hole. It may be possible to correct this discrepancy by using a finer FEA mesh near the hole.

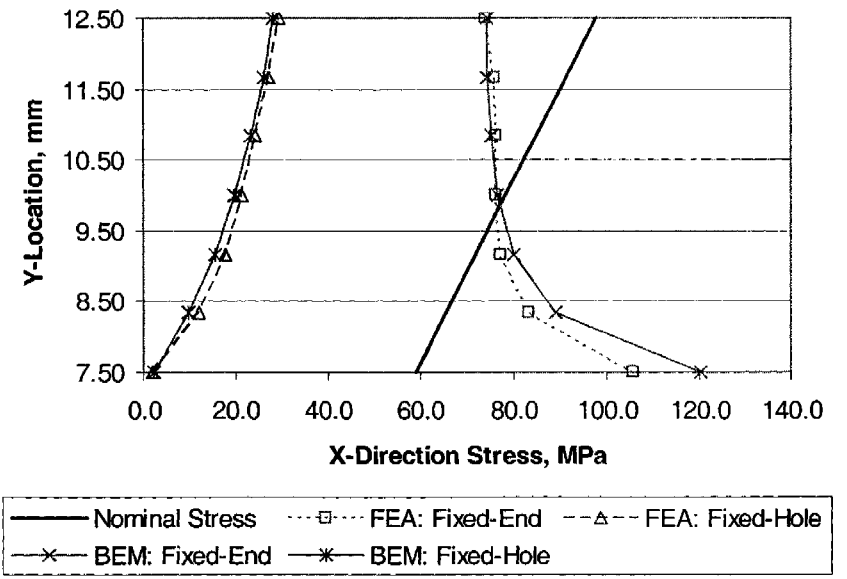

Figure 12: Comparison of stress values in the region between the top of the hole and the top of the crank arm for each method.

The results for the fixed-end BC are unexpected. Gere [1] indicates that the stress value will approach the nominal value towards the edge of the bar (see Figure 3). However, the results of this study indicate that the stress values at the edge are significantly less than the nominal stress value. The reason for this discrepancy is not clear. It may be a consequence of the type of loading (Figure 3 applies to pure bending, which is not the case here), but more than likely it suggests that Figure 3 is incorrect.

The solution for the fixed-hole boundary condition shows that the stress is very much lower than the nominal solution and confirms the conclusion reached in by the force flow analysis. The force is being transmitted directly through the interference fit into the spindle and thus does not load the region between the top of the spindle hole and the top of the crank.

A comparison of the stress values and stress concentration factors at the top edge of the hole for the fixed-end boundary condition is shown in Table 2. The FEA and BEM methods both yield results, which are consistent with the commonly accepted value ($K_t = 2$). It should be noted that this value was found by photoelastic studies (Peterson [2]).

Table 2: Comparison of the values at the top edge of the hole for the fixed-end boundary condition

Method	**Maximum Stress (MPa)**	**Stress Factor**	**Percent Difference**
Analytical	117.6	2.0	---
FEA	106.0	1.80	-9.9%
BEM	120.4	2.05	2.4%

Conclusions

This study demonstrated that the spindle hole in a bicycle crank does not create a stress concentration, as one would normally expect at a geometric discontinuity. Friction at the interference fit allows some of the applied load to be transmitted directly into the spindle and hence the stress in the region between the edge of the spindle hole and the edge of the crank is low. The force-flow analysis, BEM analysis and FEA analysis all support this conclusion. One limitation of this study was that the effects of the contact stress associated with the interference were not considered. A future study will be conducted to evaluate that effect.

References

1. Gere, J. M., "Mechanics of Materials", 5th Edition, Brooks/Cole, 2001.
2. Peterson, R. E., "Stress Concentration Factors", John Wiley & Sons, 1974.